

Arabidopsis VIRE2 INTERACTING PROTEIN2 Is Required for *Agrobacterium* T-DNA Integration in Plants ^W

Ajith Anand,^a Alexander Krichevsky,^b Sebastian Schornack,^c Thomas Lahaye,^c Tzvi Tzfira,^d Yuhong Tang,^a Vitaly Citovsky,^b and Kirankumar S. Mysore^{a,1}

^a Plant Biology Division, Samuel Roberts Noble Foundation, Ardmore, Oklahoma 73401

^b Department of Biochemistry and Cell Biology, State University of New York, Stony Brook, New York 11794

^c Institute of Genetics, Martin Luther University, D-06099 Halle (Saale), Germany

^d Department of Molecular, Cellular, and Developmental Biology, University of Michigan, Ann Arbor, Michigan 48109

***Agrobacterium tumefaciens*–mediated genetic transformation is an efficient tool for genetic engineering of plants. VirE2 is a single-stranded DNA binding *Agrobacterium* protein that is transported into the plant cell and presumably protects the T-DNA from degradation. Using a yeast two-hybrid system, we identified *Arabidopsis thaliana* VIRE2-INTERACTING PROTEIN2 (VIP2) with a NOT domain that is conserved in both plants and animals. Furthermore, we provide evidence supporting VIP2 interaction with VIP1, a basic domain/leucine zipper motif–containing protein required for nuclear import and integration of T-DNA. Virus-induced gene silencing of VIP2 in *Nicotiana benthamiana* and characterization of the *Arabidopsis vip2* mutant (At *vip2*) demonstrate that VIP2 is required for *Agrobacterium*–mediated stable transformation but not for transient transformation. Assays based upon a promoter-trap vector and quantification of T-DNA integration further confirmed VIP2 involvement in T-DNA integration. Interestingly, VIP2 transcripts were induced to a greater extent over prolonged periods after infection with a T-DNA transfer-competent *Agrobacterium* strain compared with the transfer-deficient *Agrobacterium* strain. Transcriptome analyses of At *vip2* suggest that VIP2 is likely a transcriptional regulator, and the recalcitrancy to transformation in At *vip2* is probably due to the combination of muted gene expression response upon *Agrobacterium* infection and repression of histone genes resulting in decreased T-DNA integration events.**

INTRODUCTION

Agrobacterium tumefaciens is a soil-borne phytopathogen that causes crown gall disease in plants. This disease is the manifestation of transfer, integration, and expression of oncogenes on a specific region of the T-DNA in susceptible hosts (reviewed in Gelvin, 2003; Anand and Mysore, 2006; Tzfira and Citovsky, 2006). Apart from T-DNA, several *Agrobacterium* encoded proteins, such as VirD2, VirE2, VirE3, and VirF, are also translocated into plants (Vergunst et al., 2003; Cascales and Christie, 2004; Christie, 2004). The current consensus is that *Agrobacterium* separately translocates the VirD2–T-strand and VirE2 and that the VirD2–T-strand–VirE2 complex (T-complex) assembles in the plant cell (Vergunst et al., 2000; Cascales and Christie, 2004). VirD2 remains tightly attached to the 5' end of the nicked T-DNA region, while the remaining single-stranded DNA is covered stoichiometrically with VirE2, protecting the T-strand from exonucleolytic degradation in planta. The T-complex is subsequently imported into the nucleus most likely through interactions with other host proteins, such as VIP1 (Tzfira et al., 2001) and importin α

(Ballas and Citovsky, 1997). Once inside the plant nucleus, the T-complex is stripped of its proteins probably through targeted proteolysis involving the SCF^{virF} ubiquitin complex (Tzfira et al., 2004). The T-DNA most likely relies on host DNA repair machinery for its conversion into double-stranded T-DNA intermediates and their recognition by proteins such as histone H2A (Mysore et al., 2000; Li et al., 2005a), histone H3 (Anand et al., 2007), and KU80 (Li et al., 2005b) for integration into the host chromosome.

To better characterize the functions of VirE2 in T-DNA transfer and integration, plant proteins that specifically associate with VirE2 were identified by screening the *Arabidopsis thaliana* cDNA library against VirE2 in the yeast two-hybrid system (Tzfira et al., 2001). Two VirE2-interacting proteins (VIPs) were identified and designated as VIP1 and VIP2 (Tzfira et al., 2000). Functional characterization of VIP1 through antisense and overexpression approaches implicated its requirement for T-DNA and VirE2 nuclear import via the importin α -dependent pathway (Tzfira et al., 2001; Tzfira and Citovsky, 2002). Here, we report the involvement of VIP2 in T-DNA integration. VIP2 encodes a NOT (for negative on TATA-less) domain–containing protein that interacts with VirE2 and is required for *Agrobacterium*–mediated plant transformation. VIP2 silenced and knockout plants are defective in stable T-DNA transformation but not in transient transformation. The amount of integrated T-DNAs in VIP2-silenced *Nicotiana benthamiana* plants was significantly less than in nonsilenced plants. On the basis of the above observations, we conclude that VIP2 plays an important role in *Agrobacterium*–mediated plant transformation by facilitating T-DNA integration into plant chromosomes.

¹ To whom correspondence should be addressed. E-mail ksmysore@noble.org; fax 580-224-6692.

The author responsible for distribution of materials integral to the findings presented in this article in accordance with the policy described in the Instructions for Authors (www.plantcell.org) is: Kirankumar S. Mysore (ksmysore@noble.org).

^W Online version contains Web-only data.

www.plantcell.org/cgi/doi/10.1105/tpc.106.042903

Furthermore, transcriptome analyses showed that many genes were constitutively differentially expressed in the *At vip2* knock-out, and gene expression response to *Agrobacterium* infection was muted in *At vip2* compared with wild-type *Arabidopsis* plants. These data provided insights into the possible role of VIP2 as a transcription regulator.

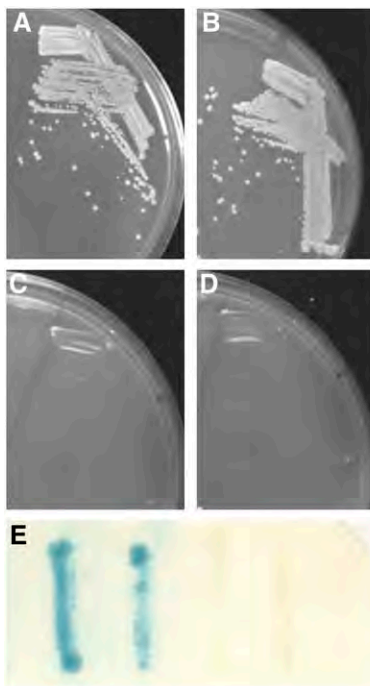
RESULTS

Identification of At VIP2

VIPs were identified using the yeast two-hybrid screen with an *Arabidopsis* cDNA library as prey and the *Agrobacterium* VirE2 protein as bait as described (Tzfira et al., 2001). Three VirE2-interacting clones belonged to the same cDNA, which was designated *At VIP2*. Coexpression of the largest clone of *At VIP2* and VirE2 (Figure 1A), but not of lamin C (Figure 1C) or topoisomerase I (Figure 1D), indicated that only *At VIP2* and VirE2 coexpression activated the HIS3 and β -galactosidase (Figure 1E) reporter genes. The interaction of *At VIP2* with VirE2 was specific because it did not occur with lamin C and DNA topoisomerase I, known as

nonspecific activators in the two-hybrid system best suited to eliminate false positive interactions (Bartel et al., 1993; Park and Sternglanz, 1998). *At VIP2* did not interact with VirD2 (data not shown) that is thought to function differently from VirE2 during the T-DNA nuclear import (Guralnick et al., 1996), which further reinforces its specific interaction. Interestingly, *At VIP2* also interacted with *At VIP1*, a previously identified VirE2-interacting protein (Tzfira et al., 2001), in the yeast two-hybrid system (Figures 1B and 1E).

Sequence analysis of the *At VIP2* cDNA predicted a single open reading frame (ORF) encoding a protein of 556 amino acids. The deduced amino acid sequence of *At VIP2* contains a conserved C-terminal domain for NOT genes (*NOT2/NOT3/NOT5*; Collart and Struhl, 1994; Oberholzer and Collart, 1998) (Figure 1F). The *VIP2* gene (At5g59710; genomic sequence of *At VIP2* carries 11 exons and 10 introns) in the *Arabidopsis* database is represented by two splice variant cDNAs (GenBank accession numbers AK117230 and AF295433; Wang and Brendel, 2006). *At VIP2* is also annotated as a transcription regulator NOT2/NOT3/NOT5 protein (GenBank accession number NM_125363). There are at least two other proteins with a NOT domain in *Arabidopsis*



F *At VIP2* MQGTLTSTRNSSMNSIPAGVQQPNGSFSSGRFASNNLPVNLSQLSHGSSHHGHSGLPNRG-
Nb VIP2 MQGTLTSTRNTAINNVPSGSGVQQSGNNLSSGGRFVPPNNLPSALSQIPQGNSSHGHSGMTSRGG

At VIP2 LNVVGNPGFSSNANGVGGSSIPGILSTAGLSNRNSVPGMGISQLLGNSGPRITNSMGNMV
Nb VIP2 TSVVGNPGYSSNTNGVGGSSIPGILPTFAAIGNRSSVPPGLGVSPILGNAGPRMTNSVGNIV

At VIP2 GGGNLGRNISSG-GLSIPGLSSRLNLAANSGSG-LNVQQNRMMGGVLPQGS-QVMSMLG
Nb VIP2 GGGNIGRSISSGAGLSVPLASRLNMANSGSGNLNVQQPNRMLSGVLPQASPVQLSMLG

At VIP2 NSYHTGGGPLSQNHVQSVNN-----MMLSDHPNDSSLFIDINDFPQLTSRPGSAGGTQGH
Nb VIP2 NSY-PAGGPLSQNHVQAIGNFNSMGLLNDVNSNDGSPFDIN-DFPQLTSRPGSAGGPQGG

At VIP2 LGSRLRQQLGVPLVQQNQEFSTIQNEDFPALPGYKGGNSEYFMDLHQKEQLHDNAMSMHS
Nb VIP2 LGSRLRQGLS-PIVQQNQEFSTIQNEDFPALPGFKGGNADYAMDPHQKEQLHDNTLSMMQQ

At VIP2 QNFMSGRSGGFNLGATYSSHRPQQQPQHTSST-----
Nb VIP2 QHFSMGRSAGFNLGGTYSSNRPPQQQLQHAPSVSSGGVVSFSNINNQDLLSLHGSDVDFQSSH

At VIP2 -----GGLQGLGLRPLSSPNVSSIG-YDQLIQYQQHQHQNSQFPVQQMSSINQ-FRD
Nb VIP2 SSYQQQGSGPPGIGLRPLNSSGTVSGIGSYDQLIQYQQHQHQNSQFRQQMSTLQPPFRD

At VIP2 SEMKSTQSEA--DPFCLLGLLDVLRNRSNPELTSALGIDLTTGLGLDLSNCGNLYKTFASP
Nb VIP2 QSLKSMQSQVADPFQMLGLLSVIRMSDDPDLTSALGIDLTTGLGLDLSNCGNLYKTFGSP

At VIP2 WTNEPAKSEVEFTVPNCYYATEPPPLTRASFKRFSYELLFYTFYSMPKDEAQLYAADELY
Nb VIP2 WSEPAKGDPEFTVPQCYAKQPPPLNQAYFSKQQLDLYIFYSMPKDEAQLYAADELY

At VIP2 ERGWFYHKELRVWFFRVG--EPLVRAATYERGTYEYLDPNFSFKTVRKEHFVIKYEELMEKR
Nb VIP2 NRGWFYHREHRLWFMRVANMEPLVKTNAYERGSYICFDPNFTWETIHKDNFVFLHCELEKR

At VIP2 PSLQL
Nb VIP2 PVLQH

Figure 1. *At VIP2*–VirE2 and *At VIP2*–*At VIP1* interactions in the Two-Hybrid System and Amino Acid Sequences of *At VIP2* and *Nb VIP2*.

(A) *At VIP2* + VirE2.

(B) *At VIP2* + *At VIP1*.

(C) *At VIP2* + human lamin C.

(D) *At VIP2* + topoisomerase I.

(E) β -Galactosidase assay. From left to right: *At VIP2* + VirE2, *At VIP2* + *At VIP1*, *At VIP2* + human lamin C, and *At VIP2* + topoisomerase I. Cells shown in (A) to (D) were grown in the absence of His, Trp, and Leu, and cells shown in (E) were grown in the absence of Trp and Leu.

(F) Multiple sequence alignment by ClustalW (1.81) of amino acid sequences of full-length proteins for *At VIP2* and *Nb VIP2*. The identical amino acids are shown in red, conserved amino acids in blue, semiconserved amino acids in green, and the divergent amino acids in black. The shaded area represents the C-terminal NOT domain between the two proteins.

(GenBank accession numbers NM_100644 and NM_121828) that have 15 and 61% similarity to At VIP2, respectively (see Supplemental Figure 1 online). The NOT domain of VIP2 is conserved among plants and animals (see Supplemental Figure 1 online).

At VIP2 Is Imported into the Plant Cell Nucleus

We examined the subcellular localization of GFP-tagged At VIP2 in epidermal cells of tobacco and onion along with another fluorescent reporter, DsRed2 (known to partition between the cell cytoplasm and the nucleus; Dietrich and Maiss, 2002; Goodin et al., 2002; Schultheiss et al., 2003). GFP-At VIP2 was imported into the nucleus of onion (*Allium cepa*) and tobacco (*Nicotiana tabacum*) cells displaying a predominantly intranuclear accumulation as determined by confocal microscopy with optical sections through the cell nucleus (see Supplemental Figures 2A and 2D online). Combined image of GFP-At VIP2 and DsRed2 fluorescence showed overlapping signal (yellow color) within the cell nucleus, confirming GFP-At VIP2 localization within the nucleus (see Supplemental Figures 2C and 2F online). These results were consistent with the previous report that showed that in transgenic *Arabidopsis* plants, the yellow fluorescent protein (YFP)-tagged At VIP2, expressed under its native promoter and terminator sequences, accumulated within the cell nucleus (Tian et al., 2004).

Silencing of Nb VIP2 by Virus-Induced Gene Silencing in *N. benthamiana* Results in Smaller Crown Galls

Due to the unavailability of an *Arabidopsis vip2* mutant at the initial stages of this study, we used a virus-induced gene silencing (VIGS)-based reverse genetics approach (Burch-Smith et al., 2004; Anand et al., 2007) to investigate whether VIP2 is required for *Agrobacterium*-mediated plant transformation. A fragment representing part of the Nb VIP2 gene (414 bp in length) was amplified by PCR from *N. benthamiana* cDNA, using primers specific to tomato (*Solanum lycopersicum*) VIP2 (SI VIP2; GenBank accession number BG130671), and cloned into tobacco rattle virus (TRV)-based VIGS vectors (Liu et al., 2002a, 2002b). The reduction of Nb VIP2 transcripts was quantified by semi-quantitative RT-PCR (see Supplemental Figure 3A online) and by real-time quantitative RT-PCR (qRT-PCR) analyses. Only 23% \pm 4% mRNA of Nb VIP2 was detected in gene-silenced plants compared with TRV:00 (virus without the insert) inoculated plants.

To test whether VIP2 is required for *Agrobacterium* infectivity, the stems of Nb VIP2-silenced, TRV:00-inoculated, and wild-type (no virus inoculation) plants were infected with oncogenic strain *A. tumefaciens* A348 as described (Anand et al., 2007). We observed relatively smaller tumors incited on the shoots of Nb VIP2-silenced plants compared with the tumors on the TRV:00-inoculated plants or wild-type plants (see Supplemental Figure 3B online).

Nb VIP2 Is Required for Stable Transformation

The ability of Nb VIP2-silenced plants to develop tumors on leaf disks was tested following inoculation with strain *A. tumefaciens* A348. Tumors were quantified by counting the number of tumors/

leaf disk and by measuring the weight of leaf disks with tumors (Figures 2A and 2B; see Supplemental Figure 4 online). The tumor-inducing capability was severely attenuated in Nb VIP2-silenced plants compared with TRV:00 and wild-type plants.

To rule out the possibility that the reduction in number of tumors produced in Nb VIP2-silenced plants could have resulted from the downregulation of genes involved in phytohormone responses, we inoculated leaf disks from the Nb VIP2-silenced and TRV:00 plants with a disarmed strain *A. tumefaciens* GV2260 containing the binary vector pCAS1 (Nam et al., 1999) that contains a *nos-bar* gene as a selectable marker. Approximately 33% of the leaf disks derived from the Nb VIP2-silenced plants survived the glufosinate ammonium (GF) selection and produced small transgenic GF-resistant calli on callus-inducing medium (CIM). In the case of TRV:00 and wild-type control plants, 100% of the leaf disks survived GF selection and produced predominantly large GF-resistant calli (Figure 2C).

Uninfected leaf disks of Nb VIP2-silenced plants were able to form calli, at an equal efficiency as that of TRV:00 plants, on non-selective CIM (Figure 2D). Thus, silencing of the VIP2 gene apparently does not interfere with essential plant cellular functions pertaining to cell division. These data clearly indicate that silencing of VIP2 in *N. benthamiana* attenuates *Agrobacterium*-mediated stable transformation.

We investigated whether the Nb VIP2-silenced plants can be efficiently transformed by *Agrobacterium*-independent transformation techniques. Leaf disks from the TRV:00 and Nb VIP2-silenced plants were biolistically transformed with 35S:*gus* (*uidA*-intron) or *Ubi:bar* constructs for transient and stable transformation, respectively. No differences were detected for the transient expression of β -glucuronidase (GUS) in the Nb VIP2-silenced plants and TRV:00-infected plants (see Supplemental Figure 5A online). No significant differences were also seen in the number of leaf disks producing GF-resistant calli on TRV:00-inoculated (76% \pm 9%) and Nb VIP2-silenced plants (67% \pm 7%). The presence of the *bar* gene in the GF-resistant calli was confirmed by PCR (data not shown). These results suggest that VIP2 gene silencing in *N. benthamiana* did not affect both transient and stable transformation by particle bombardment.

Nb VIP2-Silenced Plants Are Partially Blocked at the T-DNA Integration Step

To identify the step at which VIP2 is involved in *Agrobacterium*-mediated transformation, we inoculated leaf disks derived from the Nb VIP2-silenced *N. benthamiana* and TRV:00 plants with a disarmed strain *A. tumefaciens* GV2260 containing the binary vector pBISN1 (carries on its T-DNA a *uidA*-intron gene encoding GUS; Nam et al., 1999). The 5-bromo-4-chloro-3-indolyl β -D-glucuronide (X-Gluc) staining and GUS activity on the leaf disks of Nb VIP2-silenced plants were not significantly different than TRV:00 plants at 2 and 3 d after inoculation (DAI; Figures 3A and 3B), suggesting that there was no deficiency in transient transformation in the silenced plants. Also, no qualitative differences in the transient GUS expression were detected, when the *uidA*-intron gene was delivered by agroinfiltration, in the Nb VIP2-silenced and TRV:00 plants (see Supplemental Figure 5B online). Leaf disks from Nb VIP2-silenced plants showed less X-Gluc

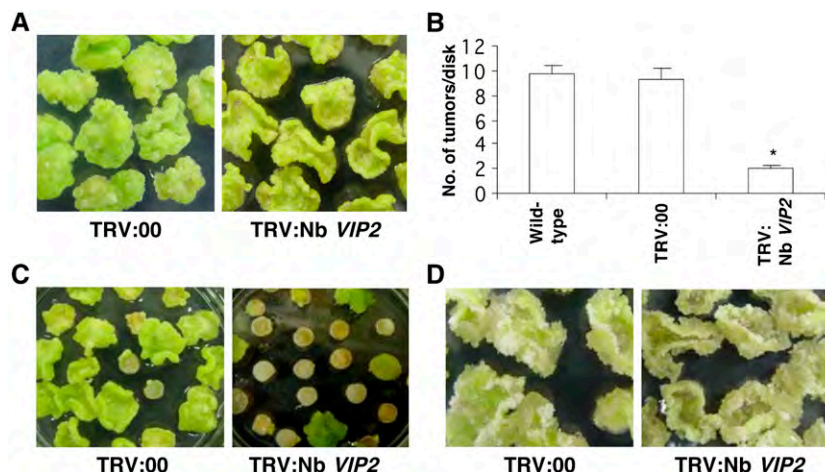


Figure 2. *Agrobacterium* Transformation Assays in Nb *VIP2*-Silenced Plants.

(A) Leaf disk tumorigenesis assay. Leaf disks of the Nb *VIP2*-silenced plants and TRV:00 (control) plants were inoculated with tumorigenic strain *A. tumefaciens* A348 and incubated on hormone-free Murashige and Skoog (MS) medium.

(B) Quantification of tumors. The number of tumors produced per leaf disk was counted 3 weeks after inoculation. Data represent the mean of two experiments with a minimum of 150 leaf disks each per treatment with their SE values shown as error bars. Asterisk denotes significant difference compared with controls using Fisher's least significant difference test at $P = 0.05$.

(C) Stable transformation assay. Leaf disks from the silenced and TRV:00 plants were infected with a nontumorigenic strain *A. tumefaciens* GV2260 harboring the binary vector pCAS1 and incubated on CIM with GF.

(D) Effect of *VIP2* gene silencing on cell division. The effect of gene silencing on cell division was evaluated by placing uninoculated leaf disks from the silenced and TRV:00 plants on a nonselective CIM. All the experiments were done with at least five biological replicates and repeated two times, and the results were consistent among the replicates. Photographs shown in **(A)**, **(C)**, and **(D)** were taken 4 weeks after *Agrobacterium* inoculation.

staining and only 61 to 65% GUS activity compared with leaf disks derived from the TRV:00 plants at 5 to 10 DAI (Figures 3A and 3B). This represents a combination of both transient and stable GUS expression. Thus, we concluded that Nb *VIP2* gene silencing partially blocked the later stages (T-DNA integration) of *Agrobacterium*-mediated transformation.

To provide additional evidence that the T-DNA integration was blocked in Nb *VIP2*-silenced plants, we inoculated the leaf disks derived from Nb *VIP2*-silenced and TRV:00 plants with a disarmed strain *A. tumefaciens* GV2260 containing the binary vector pKM1 (Mysore et al., 1998) carrying a promoterless *uidA*-intron gene and a *35S:luciferase (luc)*-intron gene within the T-DNA. Here, the expression of the *uidA* gene in plants is dependent upon T-DNA integration downstream of a plant promoter, while the *luc* gene can express transiently irrespective of T-DNA integration. Significantly less GUS activity was detected on the leaf disks of Nb *VIP2*-silenced plants at 9 to 15 DAI compared with the TRV:00 plants (Figure 3C; see Supplemental Figure 6A online). As a positive control for *Agrobacterium* infectivity, we detected the expression of the *luc* gene in the representative leaf disks derived from the same experiment for Nb *VIP2*-silenced and TRV:00 plants by semiquantitative RT-PCR (see Supplemental Figure 6B online).

To provide direct evidence for deficiency in T-DNA integration in Nb *VIP2*-silenced plants, DNA gel blot analyses (Mysore et al., 2000) were performed on high molecular weight DNA extracted from cell cultures of Nb *VIP2*-silenced and TRV:00 plants infected with a disarmed strain *A. tumefaciens* GV2260 containing

the binary vector pBISN1 (Nam et al., 1999). The differences in the amount of T-DNA, containing *uidA*-intron gene, integrated into the genomes of Nb *VIP2*-silenced and TRV:00 plants was determined by hybridizing the above-mentioned DNA blot with radiolabeled *uidA* gene. DNA from Nb *VIP2*-silenced plants showed weaker signals compared with DNA from TRV:00 plants (Figure 3D). Nb *H3*-silenced plants recently have been shown to be deficient in T-DNA integration (Anand et al., 2007). DNA from Nb *H3*-silenced plants infected with *A. tumefaciens* GV2260 containing pBISN1 was used as control. We confirmed that the plant DNA samples were free of contaminating *Agrobacterium* DNA by performing quantitative DNA PCR (qPCR) using the bacterial chromosomal gene *Atu0972* as previously described (Anand et al., 2007). The same DNA gel blot was stripped and rehybridized with the radiolabeled Nb *RAR1* gene to demonstrate that similar amounts of DNA were loaded in lanes with DNA from Nb *VIP2* and Nb *H3* cultures with respect to DNA from TRV:00 cultures (Figure 3D). Furthermore, we support the above results by quantifying the relative amount of T-DNA integrated into the genome by real-time qPCR as described (Li et al., 2005b; Anand et al., 2007) on genomic DNA extracted from the calli generated on leaf disks infected with the disarmed strain of *Agrobacterium* containing the binary vector pBISN1. The amount of PCR products specific to the *uidA* gene, determined by qPCR, was ~63% less in Nb *VIP2*-silenced plants compared with TRV:00 plants (Figure 3E). Semiquantitative PCR amplifications were also performed using primers specific to *uidA* exons bordering an intron and primers specific to a bacterial chromosome to show the

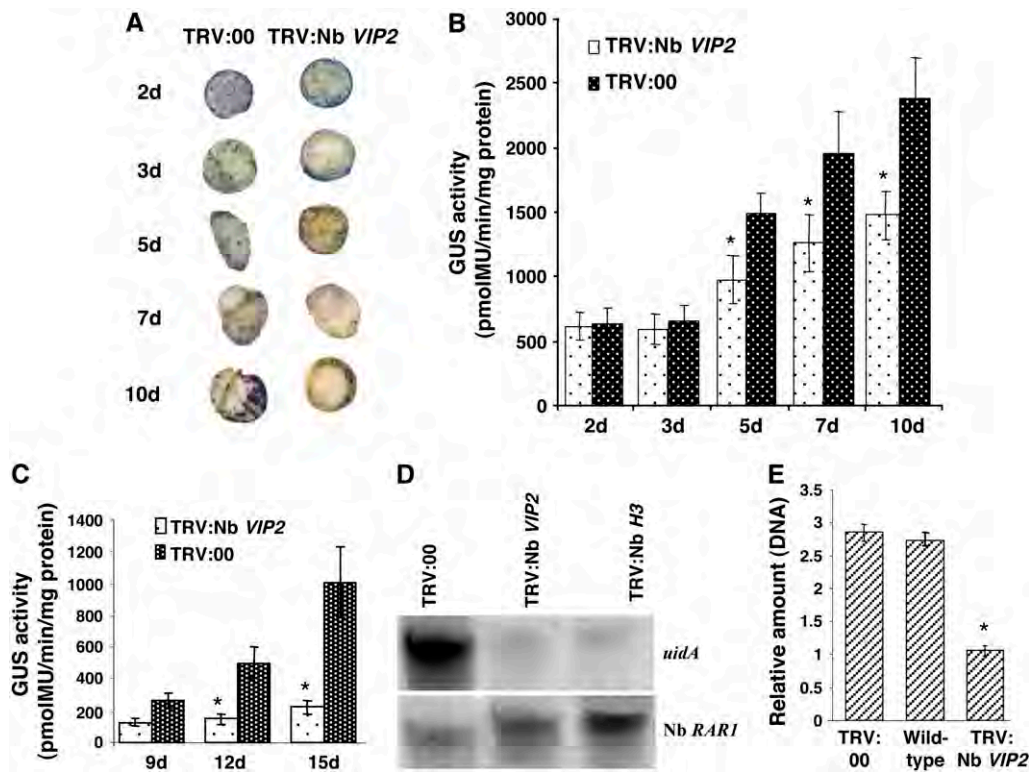


Figure 3. Transient Transformation and T-DNA Integration Assays in Nb *VIP2*-Silenced Plants.

(A) Transient transformation assay. Leaf disks of the Nb *VIP2*-silenced and TRV:00 plants were inoculated with nontumorigenic strain *A. tumefaciens* GV2260 carrying pBISN1 (has the *uidA*-intron gene within the T-DNA). The inoculated leaves were periodically collected and stained with X-Gluc.

(B) Quantification of GUS activity. Leaf disks from the experiment in **(A)** were collected periodically and were used for measuring the fluorescence of 4-methylumbelliferone (4-MU).

(C) T-DNA integration assay. Leaf disks from TRV:00 and Nb *VIP2*-silenced plants were inoculated with *Agrobacterium* strain carrying a promoterless *uidA*-intron gene and *35S:Luc*-intron gene within the T-DNA. Leaf disks were periodically collected, and GUS activity was measured as described above.

(D) T-DNA integration in the Nb *VIP2*-silenced and TRV:00-infected plants. Suspension cells were derived from the calli generated from Nb *VIP2*-silenced and TRV:00-infected leaf segments infected with the nontumorigenic strain *A. tumefaciens* GV2260 carrying pBISN1. The suspension cell lines were grown for 8 weeks in nonselective medium. Genomic DNA was isolated from these cells, subjected to electrophoresis through a 0.8% agarose gel, blotted onto a nylon membrane, and hybridized with a *uidA* gene probe. After autoradiography, the membrane was stripped and rehybridized with the Nb *RAR1* gene probe to compare the amount of DNA in each lane.

(E) Quantification of T-DNA integration. The amounts of integrated T-DNA molecules in the genomic DNA extracted from calli that were generated from leaf disks transformed with the *Agrobacterium* strain carrying the *uidA*-intron gene within the T-DNA were measured by quantitative PCR. The *uidA* gene transcripts in calli derived from Nb *VIP2*-silenced plants are represented in relative amounts in comparison to an average T-DNA amount in the calli derived from wild-type and TRV:00 plants. All the experiments were done with at least five biological replicates and repeated two times. Asterisks in **(C)** and **(E)** denote value that are significantly different between the two treatments by analysis of variance at $P = 0.05$. The data represent the average of five biological replicates in two experiments with SE values shown as error bars.

specific amplification of the integrated T-DNA molecule (see Supplemental Figure 6C online). Based on these results, we suggest that *VIP2* plays a crucial role in T-DNA integration.

Nb *VIP2* Is Induced by *Agrobacterium* Infection

The Nb *VIP2* gene was induced up to twofold 12 h after infection (HAI) with both an avirulent strain *A. tumefaciens* A136 (lacks Ti plasmid) and a T-DNA transfer competent strain *A. tumefaciens* GV2260, carrying pBISN1 when compared with the mock-inoculated *N. benthamiana* (Figure 4). Nb *VIP2* transcripts remained elevated up to 36 HAI in leaves inoculated with A136 but decreased to basal levels at 48 HAI. In the leaves infected with

GV2260, elevated transcript levels of Nb *VIP2* were maintained up to 48 HAI and were twofold to threefold more than those detected in A136-infected leaves (Figure 4). These results suggest that the transfer-competent strain of *Agrobacterium* induces *VIP2* gene expression to a greater extent than the avirulent strain.

Nb *VIP2* Interacts with VirE2 Both in Vitro and in Planta

The *N. benthamiana* gene corresponding to Nb *VIP2* was cloned by rapid amplification of cDNA ends (see Supplemental Methods online). The ORF of Nb *VIP2* is 1812 bp in length, encoding a protein of 603 amino acid residues (GenBank accession number DQ000202). Sequence alignment of the Nb *VIP2* and At *VIP2*

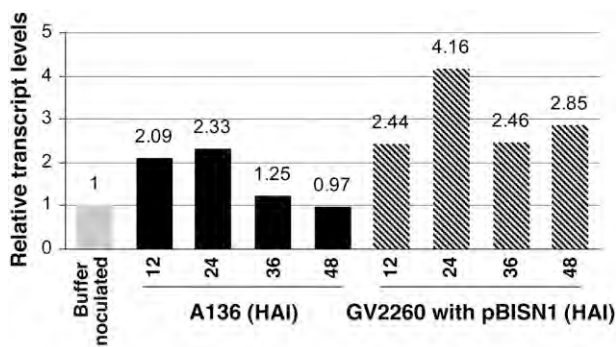


Figure 4. Differential Gene Expression of Nb *VIP2* upon Infection with *Agrobacterium*.

Individual leaves of two separate *N. benthamiana* plants were syringe (needleless) infiltrated with either an avirulent strain *Agrobacterium* A136 (lacks Ti plasmid; cannot transfer T-DNA) or a T-DNA transfer-competent strain *A. tumefaciens* GV2260 carrying pBISN1. Leaf samples from the infiltrated area were collected at different times after inoculation, and total RNA was isolated for real-time quantitative PCR. RNA from the buffer-infiltrated *N. benthamiana* leaves collected at 12 HAI was used as a calibrator to determine the relative amount of Nb *VIP2* transcripts. Samples were pooled together from two independent experiments, and the average of two technical replicates is shown.

protein sequences showed 69% sequence identity with a conserved C-terminal NOT domain (Figure 1F). Nb *VIP2* carries two in-frame insertions of five and 32 amino acids that are lacking in At *VIP2* (Figure 1F).

Nb *VIP2* also interacted with *VirE2* in a yeast two-hybrid system, and this interaction was specific since the Nb *VIP2* interaction did not occur with the nonspecific interactors such as DNA topoisomerase I and lamin C (see Supplemental Figure 7 online). We further demonstrated that Nb *VIP2* can interact with *VirE2* in planta using biomolecular fluorescence complementation (BiFC; Walter et al., 2004). BiFC vectors were modified to make it GATEWAY ready (see Methods). The interaction between N-tagged Nb *VIP2* (pSPYNE:Nb *VIP2*) and C-tagged *VirE2* (pSPYCE:*VirE2*) was observed as yellow fluorescence from the reconstitution of YFP (Figure 5). Two different controls were used for BiFC: first, we made a translational fusion of full-length *VirE2* including the stop codon (designated as *VirE2*^{*}) with cYFP in pSPYCE; second, we cloned the full-length transcription factor *TGA2* into pSPYCE. In the first control, no *VirE2*-cYFP fusion protein would be synthesized, resulting in the failure of the reconstitution of YFP fluorescence when the two interactors are brought together. The second control facilitates identification of nonspecific interaction of *VIP2* with transcription factors. YFP fluorescence was not detected in leaves coinfiltrated with pSPYNE:Nb *VIP2* and pSPYCE:*VirE2*^{*} or pSPYNE:Nb *VIP2* and pSPYCE:*TGA2* (Figure 5).

The *Arabidopsis vip2* Mutant Is Defective in T-DNA Integration but Not in Transient T-DNA Expression

Recently, we were able to identify an *Arabidopsis* T-DNA mutant line (At *vip2*; GABI_676A06; T-DNA insertion in the second exon)

(Rosso et al., 2003) (Figure 6A) that does not produce At *VIP2* transcripts (Figure 6B). To further confirm the results obtained from Nb *VIP2*-silenced plants, we performed root transformation assays on At *vip2* plants (Nam et al., 1999; Mysore et al., 2000). Upon infection with an oncogenic strain *A. tumefaciens* A208, At *vip2* produced fewer tumors (38% ± 3% of the infected roots formed tumors) compared with the wild-type plants (87% ± 5% of the infected roots formed tumors) (Figure 6C; see Supplemental Table 1 online). However, no significant differences were observed between the wild type and At *vip2* for transient GUS expression at 2 DAI (Figure 6D). Stable GUS expression in At *vip2* was only 25% ± 6% of the GUS expression observed in the wild-type plants (Figure 6D; see Supplemental Table 1 online). We also performed stable transformation assay with the strain *A. tumefaciens* GV3101 containing pCAS1. Significantly reduced numbers of GF-resistant calli were observed in the At *vip2* mutant (33% ± 1% of infected roots formed GF-resistant calli) relative to the wild-type plants (83% ± 3% of infected roots formed

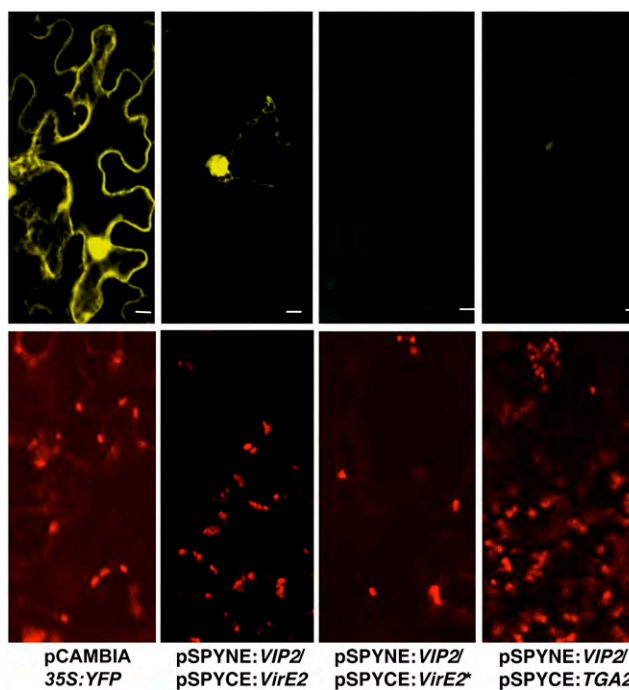


Figure 5. In Planta Interaction of Nb *VIP2* with *VirE2*.

The top panels depict the YFP fluorescence, and the bottom panels represent the epifluorescence images of epidermal leaf cells from the same leaf infiltrated with *Agrobacterium* suspension cultures harboring the indicated proteins. Individual leaves of *N. benthamiana* plants were syringe (needleless) infiltrated with *Agrobacterium* suspension cultures singly or in the following combinations: pCAMBIA1390-35S:YFP, pSPYNE:*VIP2*, pSPYCE:*VirE2*, pSPYNE:*VIP2*/pSPYCE:*VirE2*, pSPYNE:*VIP2*/pSPYCE:*TGA2*, and pSPYNE:*VIP2*/pSPYCE:*VirE2*^{*}. Wild-type 35S:YFP and fusion protein pSPYNE:*VIP2*/pSPYCE:*VirE2* are both localized to the nucleus of plant cells, while pSPYNE:*VIP2*/pSPYCE:*VirE2*^{*} carrying the *VirE2* stop codon and pSPYNE:*VIP2*/pSPYCE:*TGA2* did not produce any fluorescence. All the images are from a single confocal section. Bars = 10 μm.

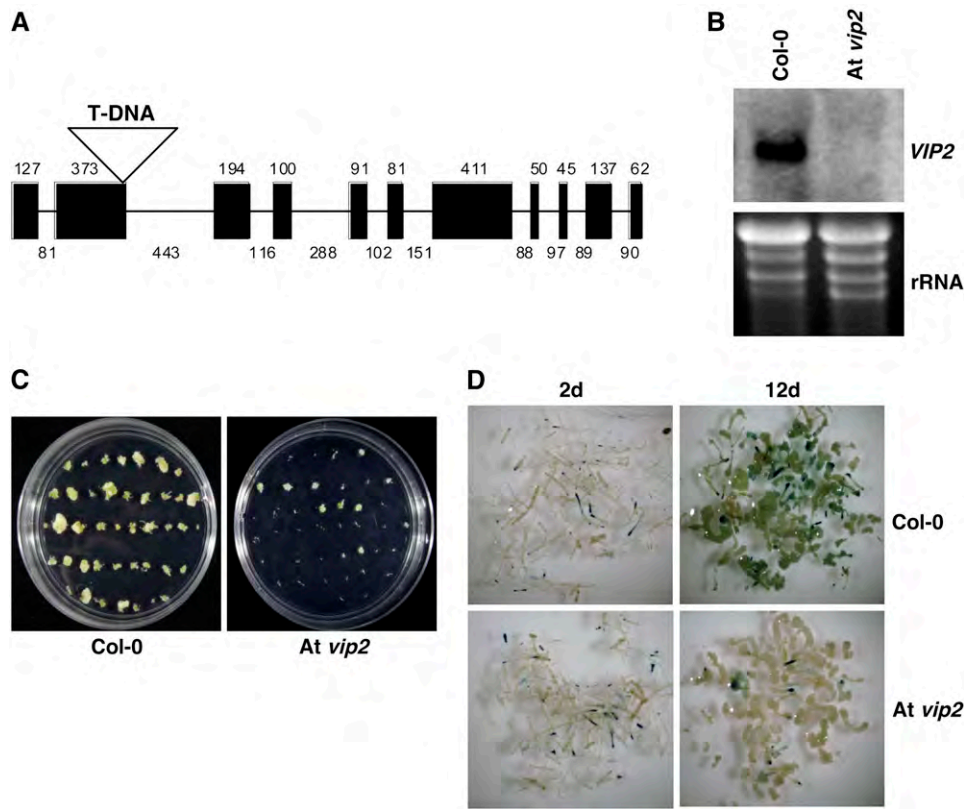


Figure 6. Identification of *At vip2* and Transformation Assays in the Mutant.

(A) The full-length genomic sequence of the *At VIP2* gene (exons are shaded) showing the T-DNA insertion in the second exon of the *Arabidopsis* T-DNA mutant line (*At vip2*; GABI_676A06).

(B) RNA gel blot analysis confirms the absence of *At VIP2* transcripts in *At vip2*. Five micrograms of RNA extracted from leaves was fractionated on a formaldehyde-agarose gel, blotted onto a nylon membrane, and probed with ^{32}P -labeled *At VIP2* gene (top panel). Ethidium bromide-stained gel showing rRNA suggests equal amounts of total RNA were loaded in each lane (bottom panel).

(C) Roots of wild-type and *vip2* mutant plants were infected with a tumorigenic strain *A. tumefaciens* A208 (nopaline strain), and tumors incited on the roots were visualized and scored 4 weeks after infection.

(D) Transient and stable GUS expression. Roots of the wild-type and *At vip2* plants were inoculated with a strain *A. tumefaciens* GV3101 carrying the *uidA*-intron gene within the T-DNA. The inoculated roots were periodically collected and stained with X-Gluc. All the experiments were repeated two times.

GF-resistant calli). Root segments derived from both the wild-type and *At vip2* mutant plants were able to form calli at similar frequencies on nonselective CIM (data not shown). These results further support the role of VIP2 in T-DNA integration in another plant species.

Transcriptome Analyses Suggest That VIP2 Plays a Role in Transcription Regulation

To gain insight on the biological role of VIP2 in plants, a comprehensive survey of global gene expression was done using the *Arabidopsis* whole-genome Affymetrix gene chip (*ATH1*) to quantify the spatio-temporal variations in transcript abundance between wild-type Columbia-0 (Col-0) and *At vip2*. Comparative analyses between Col-0 and *At vip2* showed 4241 genes to be constitutively differentially expressed with a false discovery rate (FDR) <10%. Out of the 4241 differentially expressed genes,

2157 genes had more transcript abundance in *At vip2* compared with Col-0, whereas 2084 genes had more transcript abundance in Col-0 compared with *At vip2* (see Supplemental Table 2 online). Functional classification of the 4241 differentially expressed genes indicated genes involved in a variety of functions, and the majority (28.7%) of them encode proteins of unknown function (see Supplemental Figure 8 online). These data support our hypothesis that VIP2 plays a direct or indirect role in transcription regulation of many genes. Interestingly, upon careful examination of the transcriptome data, we found a majority of the 52 genes encoding histones or histone-associated proteins to be constitutively repressed in the *At vip2* compared with Col-0 plants (Figure 7; see Supplemental Table 3 online). Although the transcript differences of some of the histone genes were less than twofold, their expression profiles were obviously different in *At vip2* and Col-0 plants (Figure 7). The exact expression values of these genes are shown in Supplemental Table 3 online. Histones

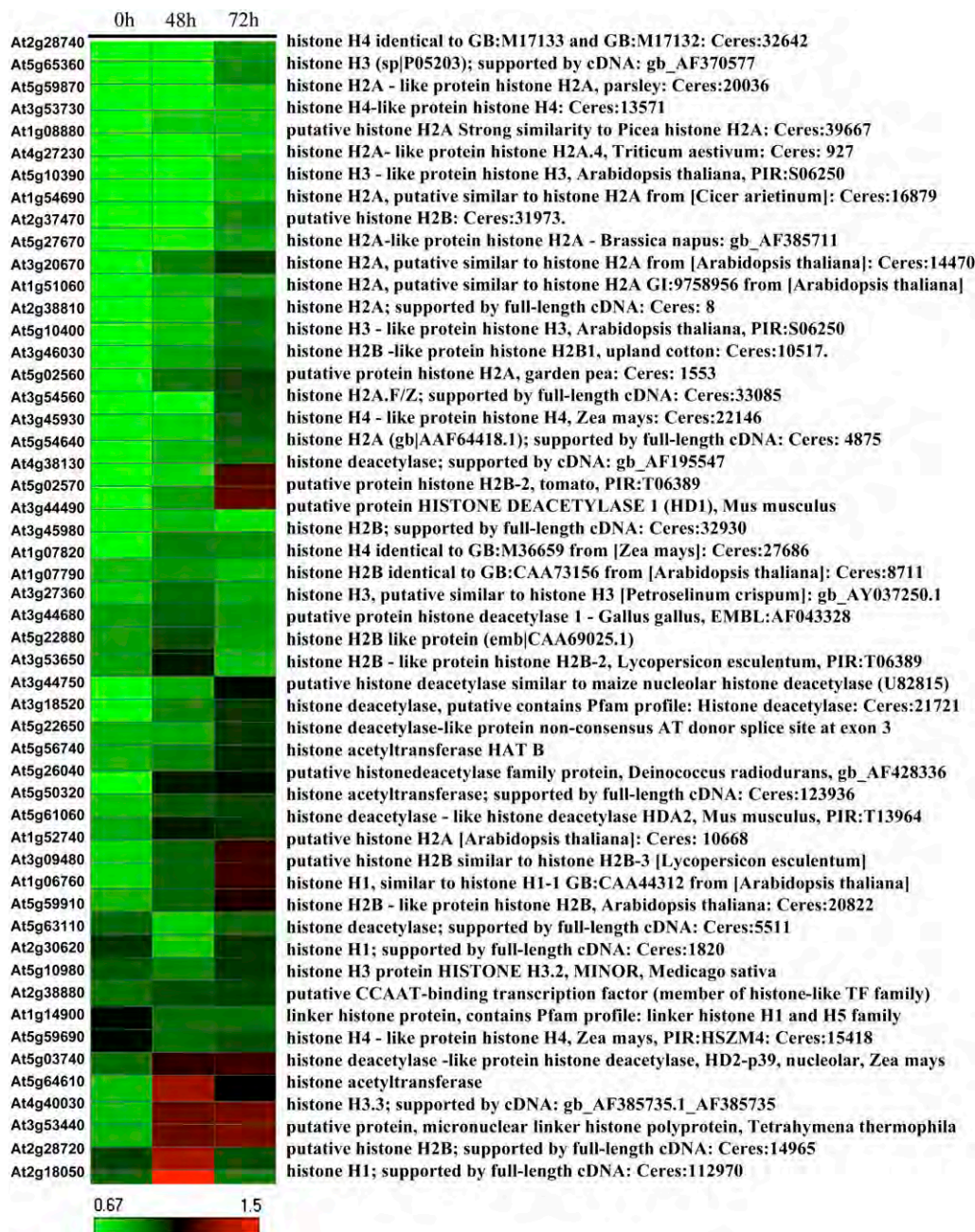


Figure 7. Expression Profile for the 52 Differentially Expressed Histone or Histone-Associated Genes Represented in the *ATH1* Gene Chips in Col-0 and *At vip2*.

Color code represents expression values of ratio between *At vip2* and Col-0, wherein red and green indicate up- and downregulation of genes, respectively. Each horizontal line displays the expression data for one gene. Data were clustered with correlation using the TIGR Multiple Experiment Viewer.

have already been implicated in *Agrobacterium*-mediated plant transformation (Mysore et al., 2000; Yi et al., 2002, 2006; Li et al., 2005a; Anand et al., 2007).

We monitored the differential expression of genes in the *At vip2* mutant and Col-0 in response to *Agrobacterium* infection by infiltrating the leaves with a disarmed strain *A. tumefaciens* GV3101

harboring the *uidA*-intron gene as described (Wroblewski et al., 2005). Strikingly, under the same selection condition, fewer genes were differentially expressed in *At vip2*, at 48 and 72 HAI, compared with the number of genes that were differentially expressed in the Col-0 plant at the same time points (see Supplemental Table 4 online). The fact that we were not able to achieve 100%

transformation in the infiltrated plants, based on the GUS histochemical staining (see Supplemental Figure 9 online), could have diluted the effect on differential gene expression upon *Agrobacterium* infection. Nevertheless, our data suggest that *At vip2* is significantly muted in its response, based on differential gene expression, to *Agrobacterium* infection. These results further validate the role of VIP2 in transcriptional regulation and *Agrobacterium*-mediated plant transformation.

Real-Time Quantitative RT-PCR Validates Microarray Data and Shows Reduced Transcript Levels of Several Histone Genes in the *At vip2* Mutant Compared with Wild-Type *Arabidopsis*

We validated the microarray results for a number of histone genes that showed differential expression between wild-type Col-0 and *At vip2*. Eight histone genes that showed less transcript abundance in *At vip2* compared with Col-0 were selected for the qRT-PCR analysis. Five members of histone H2A, namely, *HTA10* (At1g51060), *HTA3* (At1g54690), *HTA6* (At5g59870),

HTA2 (At4g27230), and *HTA11* (At3g54560); two histone H3 genes (At5g65360 and At5g10390); and one histone H4 gene (At2g28740) were selected. The transcript abundance of all eight genes tested were significantly less in *At vip2* compared with Col-0 at one or the other time point (Figure 8). For all the histone genes tested, qRT-PCR results strongly correlated with the microarray data except for *HTA3* (At1g54690), which did not show any significant difference in the expression between Col-0 and *At vip2* at 0 HAI. However, less transcripts of *HTA3* in the *At vip2* mutant compared with Col-0 were observed at 48 and 72 h after *Agrobacterium* infection. These results further imply that VIP2 may play a role in *Agrobacterium*-mediated plant transformation by modulating the expression of several plant histone genes.

DISCUSSION

Here, we report the identification of VIP2 and show that it plays an important role in *Agrobacterium*-mediated plant transformation. VIP2 protein contains a conserved C-terminal domain of

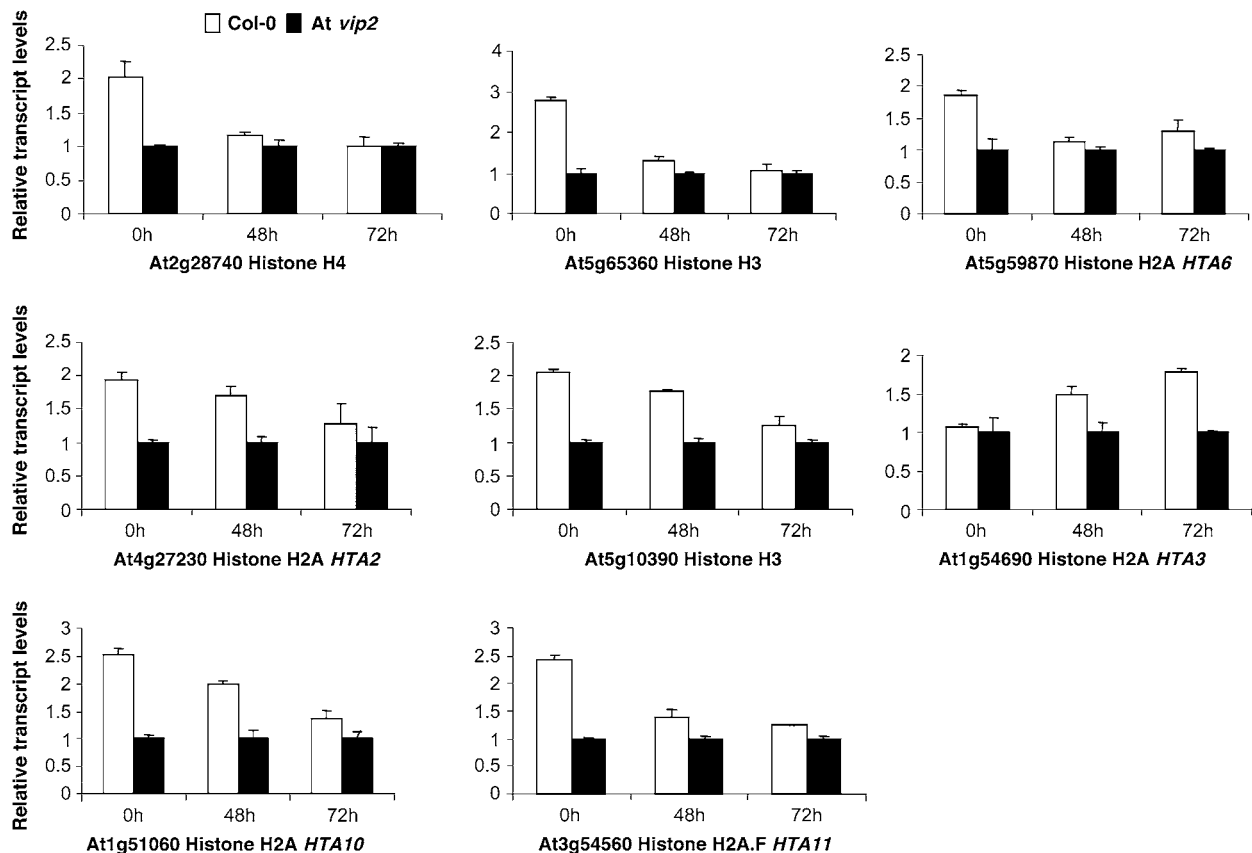


Figure 8. Validation of the Microarray Data by Real-Time qRT-PCR.

Eight different histone genes that had less transcript abundance in *At vip2* compared with Col-0, based on microarray experiments, were selected for validation. Total RNA was extracted from leaves of wild-type Col-0 and *At vip2* following agroinfiltration at 0, 48, and 72 h. The first-strand cDNA was synthesized and used for qRT-PCR using gene-specific primers (see Methods). The amount of elongation factor-1- α transcripts was determined and used for normalization. cDNA extracted from Col-0 and *At vip2* at 0 HAI was used as calibrator to obtain the relative transcript levels for each gene following agroinfiltration. The data represent the average of three biological replicates, including three technical replicates for each biological replicate with SE values shown as error bars.

NOT2/NOT3/NOT5 proteins (Figure 1F). *NOT2/NOT3/NOT5* domain-containing genes were identified from *Saccharomyces cerevisiae* via genetic screens for increased transcription from TATA-less promoters (Oberholzer and Collart, 1998; Collart, 2003). The NOT proteins are an integral component of the CCR4 (for carbon catabolite repression) transcriptional complex sharing overlapping functions (Liu et al., 1998) and are believed to be involved in both positive and negative regulation of gene expression in yeast (Collart, 2003; Collart and Timmers, 2004). The yeast Not2p and *Drosophila* Rga proteins that contain NOT domains are well studied and are thought to mediate intranuclear interactions between chromatin components and the transcriptional complex (Collart and Struhl, 1993; Frolov et al., 1998; Collart, 2003). The function of NOT domain-containing proteins in plants is not known. On the basis of its similarity to yeast and animal NOT proteins, we speculate VIP2 to be a transcriptional regulator.

The involvement of VIP2 in *Agrobacterium*-mediated plant transformation was shown using Nb *VIP2*-silenced *N. benthamiana* and an *Arabidopsis* T-DNA knockout, *At vip2*. Our observations that Nb *VIP2*-silenced and *At vip2* knockout plants were recalcitrant to *Agrobacterium*-mediated stable transformation but not to biolistic transformation further suggest that VIP2 is specifically required for *Agrobacterium*-mediated stable plant transformation. Even though the amount of stably integrated T-DNA in the Nb *VIP2*-silenced plants was significantly lower compared with the wild-type plants, the Nb *VIP2*-silenced plants did not show any deficiency for transient transformation. These results implicated a role of VIP2 in T-DNA integration. The prolonged induction of the *VIP2* transcripts by the T-DNA transfer competent strain of *Agrobacterium* compared with the induction by the avirulent strain is consistent with the hypothesis that *Agrobacterium* modulates host gene expression to facilitate the genetic transformation event (Ditt et al., 2001; Veena et al., 2003; Hwang and Gelvin, 2004). The magnitude of Nb *VIP2* induction reported is likely an underestimation due to the fact that not all cells in the infiltrated area were transformed. The specific interaction of VirE2 and Nb VIP2 was confirmed in planta by BiFC. Even though we predominantly detected YFP fluorescence in the nucleus, we seldom observed YFP fluorescence in the cytoplasm due to VirE2–Nb VIP2 interaction. It is likely that the VirE2–Nb VIP2 interaction happens in the cytoplasm and then the protein complex along with other interactors gets localized to the nucleus. Nevertheless, our data suggest that VirE2 interacts with Nb VIP2 in planta, and further studies are needed to precisely identify the cellular compartment where the initial interaction takes place.

The transcriptome analyses of wild-type *Arabidopsis* and *At vip2* identified 4241 differentially expressed genes with an FDR of 0.1, spanned across different functional groups. This was not a big surprise to us, and the data fit well with our speculation that VIP2 is likely a transcriptional regulator. This conclusion is based on circumstantial evidence, and we have not provided direct evidences to suggest its role as a transcriptional regulator. Nevertheless, *At vip2* was muted in its response (based on differential gene expression) to *Agrobacterium* infection compared with wild-type plants. This muted response of *At vip2* to *Agrobacterium* infection probably contributes to its recalcitrance to

Agrobacterium-mediated stable plant transformation. It is important to note that *At vip2* did not have any deficiency in transient transformation (2 to 3 DA); therefore, the differential gene expression that we observed at 2 and 3 d after *Agrobacterium* infection was not due to differences in transformation efficiency between *At vip2* and Col-0 plants. Strikingly, we found that transcripts of many histone genes were less abundant in *At vip2* compared with wild-type plants (Figures 7 and 8), which could be another factor contributing to the transformation recalcitrance phenotype of *At vip2*. Our data support earlier speculation that histone proteins are involved in *Agrobacterium*-mediated transformation, especially in the step of T-DNA integration (Mysore et al., 2000; Yi et al., 2002, 2006; Li et al., 2005a; Anand et al., 2007).

Based on the pfam domain prediction, VIP2 from *Arabidopsis* and *N. benthamiana* have a conserved NOT2/NOT3/NOT5 C-terminal domain, which we speculate forms complexes similar to Ccr4–Not in plants, and participates in diverse cellular functions in plant development, including chromatin remodeling, that will be addressed elsewhere. The core histones (H2A, H2B, H3, and H4) form the building blocks of the nucleosome, which are the fundamental repeating units of chromatin. Earlier observations have suggested that once inside the nucleus, the *Agrobacterium* T-DNA-associated proteins likely interact with the nucleosome assembly. VIP1, a bZIP transcription factor, was shown to interact with *Arabidopsis* histone H2A in planta (Li et al., 2005a). Furthermore, it has been shown that chromatin-associated proteins, such as histone H2A (Mysore et al., 2000), and chromatin assembly factor 1 (Endo et al., 2006; Kirik et al., 2006) play a role in T-DNA integration in plants. Core histone proteins are evolutionarily conserved and undergo posttranslational modification, implicating them in regulating gene expression (for review, see Fischle et al., 2003). The fact that NOT2/NOT3/NOT5 proteins form a nuclear complex that mediates intranuclear interactions between chromatin components and the transcriptional complex in many eukaryotes (Collart and Struhl, 1993; Frolov et al., 1998; Collart, 2003) and our finding that the histone gene transcripts are less abundant in *At vip2* further provides evidence for the biological role of VIP2 in *Agrobacterium*-mediated plant transformation. We hypothesize that *Agrobacterium* takes advantage of VIP2 to integrate its T-DNA into the plant chromosome. It is tempting to speculate that VIP1, VIP2, and VirE2 function as a multiprotein complex that plays a crucial role in T-DNA nuclear import, intranuclear transport of the T-complex, and integration of T-DNA into host genome. The above findings open up a new area of research that could be directed toward the functional characterization of VIP2 in plants and its biological relevance to plant development and transformation.

METHODS

Yeast Two-Hybrid Assay

The yeast two-hybrid assays were performed as previously described (Tzfira et al., 2001) and are detailed in the Supplemental Methods online. The Nb *VIP2* gene was cloned into pGAD424 as a *Pst*I fragment, and its product was shown to interact with pBTM116–VirE2 in a yeast two-hybrid system.

VIGS and in Planta Tumor Assay

Plant material, bacterial culture conditions, cloning of the Nb *VIP2* gene into the TRV-VIGS vector, and sequence conformation and protocols for VIGS were performed as described (Ryu et al., 2004; Anand et al., 2007) with minor modifications (see Supplemental Methods online). Shoots of the gene-silenced plants and empty vector control plants (TRV:00), 3 weeks after TRV infection, were inoculated by puncturing the stem using a needle with a suspension culture of a tumorigenic strain *Agrobacterium tumefaciens* (A348) containing the octopine type Ti plasmid (pTiA6). Tumors on shoots were observed 4 weeks after *Agrobacterium* infection.

Leaf Disk Transformation Assays

Leaf disk transformation assays were performed as described (Anand et al., 2007). Briefly, axenic leaf disks (15 to 20 for each plant) were incubated with different strains of *Agrobacterium* (see Results) for 15 min, blotted on sterile filter paper, cocultivated with the bacteria at 25°C for 2 d in the dark, and transferred onto either MS medium (Gibco-BRL) for tumorigenesis assay or to CIM (4.32 g/L MS minimal salts, 1 mL/L vitamin stock, 100 mg/L *myo*-inositol, 20 g/L glucose, 0.5 mg/L 2,4-D, 0.3 mg/mL kinetin, 5 mg/L indole-3-acetic acid, and 0.8% phytagar with antibiotics) containing cefotaxime (200 µg/mL) and tricarcillin (100 µg/mL) for stable and transient transformation assays. GF (5 µg/mL) was included in CIM for stable transformation assay. The cultures were incubated at 25.0 ± 2.0°C with a 16-h photoperiod at 70% humidity at 150 µE s⁻¹ m⁻² light intensity. Transient transformation assays (histochemical GUS staining and quantification of GUS activity) were performed as described (Jefferson et al., 1987; Anand et al., 2007).

Agrobacterium-Independent Transformation Assays

The efficacy of *Agrobacterium* independent transformation methods in the Nb *VIP2*-silenced leaves was tested by particle bombardment. DNA (1 µg) was adsorbed onto 10 mg of 1-µm gold particles (Bio-Rad) and bombarded at 150 p.s.i. into the leaf epidermis of greenhouse-grown *Nicotiana benthamiana* plants, followed by incubation for 24 to 48 h at 25°C in dark. For the transient transformation assay, leaf disks from the TRV:00-inoculated and Nb *vip2*-silenced plants were biolistically transformed with a 35S:*uidA* (pAHC20) construct. Bombarded leaves were stained with X-Gluc staining solution (50 mM NaH₂PO₄, 10 mM Na₂-EDTA, 300 mM mannitol, and 2 mM X-Gluc, pH 7.0) 48 to 72 h after bombardment and viewed under a Bio-Rad confocal microscope for GUS-expressing spots. For the stable transformation assay, the leaf disks from the TRV:00 and Nb *VIP2*-silenced plants were biolistically transformed with *Ubi:bar* (pAHC20 cassette). The transformed leaf disks were selected on media supplemented with GF for 8 weeks, and the presence of the *bar* gene was detected by PCR in a few representative GF-resistant calli as described earlier (Anand et al., 2003b).

RNA Extraction, PCR, T-DNA Integration Assay, and Differential Gene Expression

RNA extraction, first-strand cDNA synthesis, semiquantitative RT-PCR, and qRT-PCR were performed using standard protocols as described (Ryu et al., 2004; see Supplemental Methods online). The RNA gel blot analyses were performed using standard protocols (Anand et al., 2003a) on total RNA extracted from leaves of Col-0 and the At *vip2* mutant. For the T-DNA integration assay, we performed DNA gel blot analysis (Mysore et al., 2000) on the genomic DNA extracted from suspension cell lines generated from the calli produced on nonselective medium by leaf disks of Nb *VIP2*-silenced plants and TRV:00 plants infected with disarmed strain *A. tumefaciens* GV2260 carrying pBISN1 (see Results). Suspension cells were cultured for 8 weeks, in the presence of timentin, by periodic

transferring into fresh media to remove bacterial contamination. Representative suspension cells were collected and stained with X-Gluc solution to check for the presence and expression of the *uidA*-gene in the transgenic cells. The DNA gel blots were hybridized with radiolabeled probes of the *uidA* and Nb *RAR1* genes for detecting the integrated T-DNA and as control for DNA loading, respectively. For real-time quantification of integrated T-DNA, genomic DNA was extracted from calli (collected from a pool of two independent experiments, with five biological replicates each) produced on leaf disks of Nb *VIP2*-silenced and TRV:00 plants that were transformed with strain *A. tumefaciens* GV2260 carrying pBISN1. Calli were washed with dimethyl sulfoxide (15% [w/v]) several times by vortexing to remove any attached bacteria, and DNA was extracted using DNAzol (Invitrogen) according to the manufacturer's instructions. Quantitative DNA PCRs were performed on duplicate DNA samples using the *GUS* gene and *Agrobacterium* chromosomal gene (*Atu0792*) specific primers (for primer details, see Anand et al., 2007) to check for the presence of the *uidA* gene and bacterial DNA contamination. Duplicate samples were analyzed by qPCR with the primers GUS-FP (5'-AGG-TGCACGGGAATATTCG-3') and GUS-RP (5'-ACGCGTCGGGTCGAGTT-3') to determine the abundance of integrated T-DNA. As a loading control for silenced and nonsilenced plants, parallel qPCR reactions using Nb *Ef1α* primers Nb *Ef1F* (5'-TGAGGCTCTTGACCAGATTAATGA-3') and Nb *Ef1R* (5'-GTAAACATCTGAAGTGAAGACGTA-3') were performed.

For differential gene expression analyses of Nb *VIP2*, individual leaves of two separate *N. benthamiana* plants were infiltrated (using a needleless syringe) with an avirulent strain *Agrobacterium* A136 or a T-DNA transfer competent strain *A. tumefaciens* GV2260 carrying pBISN1 or the infiltration buffer. Samples were collected at different time points after inoculation and were subjected to qRT-PCR using primers Nb *VIP2F* (5'-AAGGTGG-GAATGCTGATTATGC-3') and Nb *VIP2R* (5'-TCTTCCCATTGAGAAG-TGTTGCT-3'), in parallel with Nb *Ef1α* primers as loading control. The experiments were repeated twice.

Characterization of At *vip2*

Seeds of *Arabidopsis thaliana* wild-type Col-0 and T-DNA insertion mutant GABI_676A06 (At *vip2*) were germinated, and the roots were subjected to transient and stable *Agrobacterium*-mediated transformation assays as described (Nam et al., 1999; Zhu et al., 2003). RNA gel blot analyses were performed on RNA extracted from homozygous At *vip2* plants and wild-type Col-0 plants using the radiolabeled probe of the At *VIP2* gene. RT-PCR reactions were performed on cDNAs prepared from the mutant using primer combinations (At *VIP2F*, 5'-TGGTTCGGGCAGATCGTTTAC-TGC-3'; At *VIP2R*, 5'-GCAAGCTTGGTCTCTTTTC-3') to determine the presence of At *VIP2* transcript. In vitro tumorigenesis assays were performed on the axenic root segments by infecting with oncogenic strain *A. tumefaciens* A208 containing a nopaline-type Ti plasmid (pTIT37), cocultivated for 48 h in dark at room temperature, transferred to a hormone-free MS media supplemented with cefotaxime and tricarcillin, and the tumor numbers and phenotypes were recorded 4 to 5 weeks after infection. Transient and stable GUS expression assays and the GF-resistant calli assay were performed as detailed earlier (Li et al., 2005b) using the disarmed strain *A. tumefaciens* GV3101 containing either pBISN1 or pCAS1.

Expression Profiling in the *vip2* Mutant in Response to *Agrobacterium* Infection

The Affymetrix microarrays (*Arabidopsis ATH1* genome array) were used in the expression profiling study involving At *vip2* and Col-0 plants. The wild-type Col-0 and At *vip2* mutant plants were syringe (needleless) infiltrated with the disarmed strain *A. tumefaciens* GV3101 (OD₆₀₀ ~0.2). Samples were collected at 0, 48, and 72 HAI based on the previous report (Ditt et al., 2006) showing strong differential gene expression at 48 HAI in *Arabidopsis* suspension cell cultures following *Agrobacterium* infection.

Preliminary experiments on agroinfiltration in *Arabidopsis* indicated that the earliest GUS expression was observed at 48 HAI, with the GUS expression even stronger at 72 HAI, which is indicative of higher transformation frequency. Leaf samples were individually pooled from the infected plants (10 plants for each time point) for RNA extraction, and few representative leaves were stained with X-Gluc to confirm GUS expression. Total RNA was extracted from two independent biological replicates as described earlier (Ryu et al., 2004). RNA was further cleaned with the RNeasy mini kit (Qiagen) following the manufacturer's instructions, and the quality check was performed using the Bioanalyzer 2100 (Agilent Technologies). Affymetrix chip labeling, hybridization, and scanning procedures followed the instructions provided in the Affymetrix manual (www.affymetrix.com/support/technical/manual/expression_manual.affx).

Data Analysis, Gene Clustering, and Validation of the Microarray Data

Leaf disk transformation data were subjected to analysis of variance using JMP software version 4.0.4 (SAS Institute) or by analysis of variance. When a significant result using *F*-test was obtained at $P = 0.05$, separation of treatment means was determined by Fisher's protected least significant difference.

To obtain genes differentially expressed between the wild type and mutant, pairwise comparisons were performed for microarray data obtained from Col-0 and At *vip2* at the same treatment conditions. Genes responsive to *Agrobacterium* treatment in both Col-0 and At *vip2* were identified by comparing the treated samples with their 0 h control accordingly. For each comparison, the normalized data were imported into an Excel sheet, and differential genes were selected using the Associative Analysis algorithm developed by Dozmorov and Centola (2003). In this analysis, the Bonferroni adjusted *P* value threshold for Student's *t* test was set at $0.05/N$, $n = 22,000$, the number of probe sets in the reference group (Dozmorov and Centola, 2003). The corrected *P* value ensures that the overall false positive among the multiple comparisons are controlled under 0.05. To account for multiple hypotheses testing, *Q* values, an estimation of FDR, were also calculated for each probe set using EDGE software (<http://www.biostat.washington.edu/software/jstorey/edge/>; Storey and Tibshirani, 2003). The *Q* value for a particular probe set reflects the proportion of false positives incurred among all probe sets as or more significant than the one being measured (Storey and Tibshirani, 2003). For comparative gene expression analyses of histone and histone-related genes between Col-0 and the At *vip2* mutant following *Agrobacterium* treatment, all 52 histones and histone-related genes known to be expressed (having the presence of calli in both replicates) were clustered and visualized using TIGR Multiple Experiment Viewer (<http://www.tm4.org/mev.html>).

A few differentially regulated histone genes identified from the transcriptome analysis were selected for validation of the results by qRT-PCR (see Supplemental Table 5 online for primer details). The data from two of the biological replicates used for microarray analysis and an independent third biological replicate each with three technical replicates were analyzed to quantify the relative transcript levels in At *vip2* and Col-0 plants.

BiFC Assay

Agrobacterium binary BiFC vectors (Walter et al., 2004), pSPYNE-35S and pSPYCE-35S with YFP dissected into two parts (the N-terminal [nYFP] and the C-terminal [cYFP]) were used to generate GATEWAY-compatible derivatives. A blunt-end GATEWAY cassette, reading frame B (Invitrogen), was inserted into the *EcoRV* site of pBluescript SKII+ (Stratagene) to obtain pBGB-EH. Subsequently, an *XbaI-XhoI* fragment of pBGB-EH was transferred into the *XbaI-XhoI* sites of pSPYNE-35S and pSPYCE-35S to obtain pSPYNE-35S_GW and pSPYCE-35S_GW, respectively. For fusion protein analyses, the full-length Nb *VIP2* ORF was

cloned into the nYFP construct (pSPYNE:*VIP2*) and the translational fusion of *VirE2* into the cYFP construct with (pSPYCE:*VirE2*^{*}) and without (pSPYCE:*VirE2*) the stop codon. We also cloned the transcriptional factor *TGA2* gene into the cYFP construct (pSPYCE:*TGA2*). These constructs were transformed into strain *A. tumefaciens* GV2260 by electroporation. We used pCambia1390 harboring the *35S::YFP* in GV2260 as a positive control. All the strains of *Agrobacterium* were grown in Luria-Bertani media under appropriate antibiotics overnight, induced with acetosyringone (100 μ g/mL) for 4 h at room temperature. *Agrobacterium* strains containing individual constructs were mixed at a 1:1 ratio and infiltrated (~ 1.0 OD) into the leaves of 3- to 4-week-old *N. benthamiana* plants. The infiltrated plants were placed in the dark for 72 h, and leaf sections were examined by a Leica TCS SP2 AOBs confocal laser scanning microscope with the samples excited at 514 nm at 72 HAI. These experiments were repeated twice.

Accession Numbers

Sequence data from this article can be found in the GenBank/EMBL data libraries under accession numbers AF295433 (At *VIP2*) and DQ000202 (Nb *VIP2*).

Supplemental Data

The following materials are available in the online version of this article.

- Supplemental Figure 1.** Alignment of Proteins with the NOT Domain.
- Supplemental Figure 2.** Nuclear Localization of At *VIP2* in Plant Cells.
- Supplemental Figure 3.** Semiquantitative RT-PCR Analyses and in Planta Tumor Assays.
- Supplemental Figure 4.** Quantification of Tumors in Nb *VIP2*-Silenced Plants.
- Supplemental Figure 5.** Nb *VIP2*-Silenced Plants Transformed by Alternate Methods.
- Supplemental Figure 6.** T-DNA Integration Assay.
- Supplemental Figure 7.** Nb *Vip2*-*VirE2* Interaction.
- Supplemental Figure 8.** Classification of the 4241 Differentially Expressed Genes.
- Supplemental Figure 9.** Transient Expression of the *uidA*-Intron Gene in Leaves of *Arabidopsis* Plants.
- Supplemental Table 1.** Quantitative Analyses of Transient and Stable Transformations in *Arabidopsis* At *vip2* Mutant and Wild-Type Plants.
- Supplemental Table 2.** Differentially Expressed Genes between Col-0 and At *vip2* at the Same Treatment Conditions and between 0 h Control and Treatments in Either Col-0 or At *vip2*.
- Supplemental Table 3.** Differentially Expressed Histone and Histone-Associated Genes in At *vip2* and Col-0 in Response to *Agrobacterium* Infection.
- Supplemental Table 4.** Differential Gene Expression in the Wild-Type Col-0 and the At *vip2* Mutant in Response to *Agrobacterium* Infection.
- Supplemental Table 5.** Primer Sequences of Genes Used for Revalidation of the Microarray Data by qRT-PCR.
- Supplemental Methods.**

ACKNOWLEDGMENTS

We thank S. Gelvin, S. Uppalapati, and M. Udvardi for critical reading of the manuscript. We also thank S.P. Dinesh-Kumar for providing GATEWAY

ready TRV-VIGS vectors, Stan Gelvin for many strains of *Agrobacterium*, Miki Hartwell and Candice Jones for their assistance with *in vitro* assays, and Stacy Allen for his assistance with the microarray experiments. This work was supported by Noble Foundation and by National Science Foundation Award 0445799 (K.S.M.). The work in the V.C. laboratory is supported by grants from the National Institutes of Health, the National Science Foundation, the USDA, the U.S.–Israel Binational Agricultural Research and Development Fund, and the U.S.–Israel Binational Science Foundation. The confocal system used at the Noble Foundation was from an equipment grant from the National Science Foundation (DBI 0400580).

Received March 30, 2006; revised February 4, 2007; accepted April 27, 2007; published May 11, 2007.

REFERENCES

- Anand, A., and Mysore, K.S.** (2006). *Agrobacterium*-biology and crown gall disease. In *Plant-Associated Bacteria*, S.S. Gnanamanickam, ed (Dordrecht, The Netherlands: Springer Science), pp. 359–384.
- Anand, A., Trick, H.N., Gill, B.S., and Muthukrishnan, S.** (2003b). Stable transgene expression and random gene silencing in wheat. *Plant Biotechnol. J.* **1**: 241–252.
- Anand, A., Zarir, V., Ryu, C.M., Kang, L., del-Pozo, O., Martin, G.B., and Mysore, K.S.** (2007). Identification of plant genes involved in *Agrobacterium*-mediated transformation by using virus-induced gene silencing as a functional genomics tool. *Mol. Plant Microbe Interact.* **20**: 41–52.
- Anand, A., Zhou, T., Trick, H.N., Gill, B.S., Bockus, W.W., and Muthukrishnan, S.** (2003a). Greenhouse and field testing of transgenic wheat plants stably expressing genes for thaumatin-like protein, chitinase and glucanase against *Fusarium graminearum*. *J. Exp. Bot.* **54**: 1101–1111.
- Ballas, N., and Citovsky, V.** (1997). Nuclear localization signal binding protein from *Arabidopsis* mediates nuclear import of *Agrobacterium* VirD2 protein. *Proc. Natl. Acad. Sci. USA* **94**: 10723–10728.
- Bartel, P., Chien, C., Sternglanz, R., and Fields, S.** (1993). Elimination of false positives that arise in using the two-hybrid system. *Biotechniques* **14**: 920–924.
- Burch-Smith, T.M., Anderson, J.C., Martin, G.B., and Dinesh-Kumar, S.P.** (2004). Applications and advantages of virus-induced gene silencing for gene function studies in plants. *Plant J.* **39**: 734–746.
- Cascales, E., and Christie, P.J.** (2004). Definition of a bacterial type IV secretion pathway for a DNA substrate. *Science* **304**: 1170–1173.
- Christie, P.J.** (2004). Type IV secretion: The *Agrobacterium* VirB/D4 and related conjugation systems. *Biochim. Biophys. Acta* **1694**: 219–234.
- Collart, M.A.** (2003). Global control of gene expression in yeast by the Ccr4-Not complex. *Gene* **313**: 1–16.
- Collart, M.A., and Struhl, K.** (1993). CDC39 an essential nuclear protein that negatively regulates transcription and differentially affects the constitutive and inducible *his3* promoters. *EMBO J.* **12**: 177–186.
- Collart, M.A., and Struhl, K.** (1994). *NOT1* (*CDC39*), *NOT2* (*CDC35*), *NOT3* and *NOT4* encode a global-negative regulator of transcription that differentially affects TATA-element utilization. *Genes Dev.* **8**: 525–537.
- Collart, M.A., and Timmers, H.T.** (2004). The eukaryotic Ccr4-Not complex: A regulatory platform integrating mRNA metabolism with cellular signaling pathways? *Prog. Nucleic Acid Res. Mol. Biol.* **77**: 289–322.
- Dietrich, C., and Maiss, E.** (2002). Red fluorescent protein DsRed from *Discosoma* sp. as a reporter protein in higher plants. *Biotechniques* **32**: 286–293.
- Ditt, R.F., Kerr, F.K., de Figueiredo, P., Delrow, J., Comai, L., and Nester, E.W.** (2006). The *Arabidopsis thaliana* transcriptome in response to *Agrobacterium tumefaciens*. *Mol. Plant Microbe Interact.* **19**: 665–681.
- Ditt, R.F., Nester, E.W., and Comai, L.** (2001). Plant gene expression response to *Agrobacterium tumefaciens*. *Proc. Natl. Acad. Sci. USA* **98**: 10954–10959.
- Dozmorov, I., and Centola, M.** (2003). An associative analysis of gene expression array data. *Bioinformatics* **22**: 204–211.
- Endo, M., Ishikawa, Y., Osakabe, K., Nakayama, S., Kaya, H., Araki, T., Shibahara, K., Abe, K., Ichikawa, H., Valentine, L., Hohn, B., and Toki, S.** (2006). Increased frequency of homologous recombination and T-DNA integration in *Arabidopsis* CAF-1 mutants. *EMBO J.* **25**: 5579–5590.
- Fischle, W., Wang, Y., and Allis, C.D.** (2003). Histone and chromatin cross-talk. *Curr. Opin. Cell Biol.* **15**: 172–183.
- Frolov, M.V., Benevolenskaya, E.V., and Birchler, J.A.** (1998). Regena (Rga), a *Drosophila* homolog of the global negative transcriptional regulator CDC36 (NOT2) from yeast, modifies gene expression and suppresses position effect variegation. *Genetics* **148**: 317–330.
- Gelvin, S.B.** (2003). *Agrobacterium*-mediated plant transformation: The biology behind the “gene-jockeying” tool. *Microbiol. Mol. Biol. Rev.* **67**: 16–37.
- Goodin, M.M., Dietzgen, R.G., Schichnes, D., Ruzin, S., and Jackson, A.O.** (2002). pGD vectors: Versatile tools for the expression of green and red fluorescent protein fusions in agroinfiltrated plant leaves. *Plant J.* **31**: 375–383.
- Guralnick, B., Thomsen, G., and Citovsky, V.** (1996). Transport of DNA into the nuclei of *Xenopus* oocytes by a modified VirE2 protein of *Agrobacterium*. *Plant Cell* **8**: 363–373.
- Hwang, H.-H., and Gelvin, S.B.** (2004). Plant proteins that interact with VirB2, the *Agrobacterium tumefaciens* pilin protein, mediate plant transformation. *Plant Cell* **16**: 3148–3167.
- Jefferson, R.A., Kavanagh, T.A., and Bevan, M.W.** (1987). GUS fusions: β -Glucuronidase as a sensitive and versatile gene fusion marker in higher plants. *EMBO J.* **6**: 901–907.
- Kirik, A., Pecinka, A., Wendeler, E., and Reiss, B.** (2006). The chromatin assembly factor subunit FASCIATA1 is involved in homologous recombination in plants. *Plant Cell* **18**: 2431–2442.
- Li, J., Krichevsky, A., Vaidya, M., Tzfira, T., and Citovsky, V.** (2005a). Uncoupling of the functions of the *Arabidopsis* VIP1 protein in transient and stable plant genetic transformation by *Agrobacterium*. *Proc. Natl. Acad. Sci. USA* **102**: 5733–5738.
- Li, J., Vaidya, M., White, C., Vainstein, A., Citovsky, V., and Tzfira, T.** (2005b). Involvement of KU80 in T-DNA integration in plant cells. *Proc. Natl. Acad. Sci. USA* **102**: 19231–19236.
- Liu, H.-Y., Badarinarayana, V., Audino, D.C., Rappsilber, J., Mann, M., and Denis, C.L.** (1998). The NOT proteins are part of the CCR4 transcriptional complex and affect gene expression both positively and negatively. *EMBO J.* **17**: 1096–1106.
- Liu, Y., Schiff, M., and Dinesh-Kumar, P.** (2002a). Virus-induced gene silencing in tomato. *Plant J.* **31**: 777–786.
- Liu, Y., Schiff, M., Marathe, R., and Dinesh-Kumar, P.** (2002b). Tobacco *Rar1*, *EDS1* and *NPR1/NIM1* like genes are required for N-mediated resistance to tobacco mosaic virus. *Plant J.* **30**: 415–429.
- Mysore, K.S., Bassuner, B., Deng, X.B., Darbinian, N.S., Motchoulski, A., Ream, W., and Gelvin, S.B.** (1998). Role of the *Agrobacterium tumefaciens* VirD2 protein in T-DNA transfer and integration. *Mol. Plant Microbe Interact.* **11**: 668–683.
- Mysore, K.S., Nam, J., and Gelvin, S.B.** (2000). An *Arabidopsis* histone H2A mutant is deficient in *Agrobacterium* T-DNA integration. *Proc. Natl. Acad. Sci. USA* **97**: 948–953.

- Nam, J., Mysore, K.S., Zheng, C., Knue, M.K., Matthysse, A.G., and Gelvin, G.B.** (1999). Identification of T-DNA tagged *Arabidopsis* mutants that are resistant to transformation by *Agrobacterium*. *Mol. Gen. Genet.* **261**: 429–438.
- Oberholzer, U., and Collart, M.A.** (1998). Characterization of NOT5 that encodes a new component of the Not protein complex. *Gene* **207**: 61–69.
- Park, H., and Sternglanz, R.** (1998). Two separate conserved domains of eukaryotic DNA topoisomerase I bind to each other and reconstitute enzymatic activity. *Chromosoma* **107**: 211–215.
- Rosso, M.G., Li, Y., Strizhov, N., Reiss, B., Dekker, K., and Weisshaar, B.** (2003). An *Arabidopsis thaliana* T-DNA mutagenized population (GABI-Kat) for flanking sequence tag-based reverse genetics. *Plant Mol. Biol.* **53**: 247–259.
- Ryu, C.-M., Anand, A., Kang, L., and Mysore, K.S.** (2004). Agrodrench: A novel and effective agroinoculation method for virus-induced gene silencing in roots and diverse Solanaceous species. *Plant J.* **40**: 322–331.
- Schultheiss, H., Dechert, C., Kogel, K.H., and Hückelhoven, R.** (2003). Functional analysis of barely RAC/ROP G-protein family members in susceptibility to the powdery mildew fungus. *Plant J.* **36**: 589–601.
- Storey, J.D., and Tibshirani, R.** (2003). Statistical significance for genome-wide studies. *Proc. Natl. Acad. Sci. USA* **100**: 9440–9445.
- Tian, G.-W., et al.** (2004). High-throughput fluorescent tagging of full-length *Arabidopsis* gene products in planta. *Plant Physiol.* **135**: 25–38.
- Tzfira, T., and Citovsky, V.** (2002). Partners-in-infection: Host proteins involved in the transformation of plant cells by *Agrobacterium*. *Trends Cell Biol.* **12**: 121–129.
- Tzfira, T., and Citovsky, V.** (2006). *Agrobacterium*-mediated genetic transformation of plants: Biology and biotechnology. *Curr. Opin. Biotechnol.* **17**: 147–154.
- Tzfira, T., Li, J., Lacroix, B., and Citovsky, V.** (2004). *Agrobacterium* T-DNA integration: Molecules and models. *Trends Genet.* **20**: 375–383.
- Tzfira, T., Rhee, Y., Chen, M.-H., Kunik, T., and Citovsky, V.** (2000). Nucleic acid transport in plant-microbe interactions: The molecules that walk through the Walls. *Annu. Rev. Microbiol.* **54**: 187–219.
- Tzfira, T., Vaidya, M., and Citovsky, V.** (2001). VIP1, an *Arabidopsis* protein that interacts with *Agrobacterium* VirE2, is involved in VirE2 nuclear import and *Agrobacterium* infectivity. *EMBO J.* **20**: 3596–3607.
- Veena, Jiang, H., Doerge, R.W., and Gelvin, S.B.** (2003). Transfer of T-DNA and Vir proteins to plant cells by *Agrobacterium tumefaciens* induces expression of host genes involved in mediating transformation and suppresses host defense gene expression. *Plant J.* **35**: 219–226.
- Vergunst, A.C., Schrammeijer, B., den Dulk-Ras, A., de Vlaam, C.M.T., Regensburg-Tuink, T.J., and Hooykaas, P.J.** (2000). VirB/D4-dependent protein translocation from *Agrobacterium* into plant cells. *Science* **290**: 979–982.
- Vergunst, A.C., van Lier, M.C.M., den Dulk-Ras, A., and Hooykaas, P.J.** (2003). Recognition of the *Agrobacterium* VirE2 translocation signal by the VirB/D4 transport system does not require VirE1. *Plant Physiol.* **133**: 978–988.
- Walter, M., Chaban, C., Schutze, K., Batistic, O., Weckermann, K., Nake, C., Blazevic, D., Grefen, C., Schumacher, K., Oecking, C., Harter, K., and Kudla, J.** (2004). Visualization of protein interactions in living plant cells using bimolecular fluorescence complementation. *Plant J.* **40**: 428–438.
- Wang, B.-B., and Brendel, V.** (2006). Genomewide comparative analysis of alternative splicing in plants. *Proc. Natl. Acad. Sci. USA* **103**: 7175–7180.
- Wroblewski, T., Tomczak, A., and Micheltore, R.** (2005). Optimization of *Agrobacterium*-mediated transient assays of gene expression in lettuce, tomato and *Arabidopsis*. *Plant Biotechnol. J.* **3**: 259–273.
- Yi, H., Sardesai, N., Fujinuma, T., Chan, C.W., Veena, and Gelvin, S.B.** (2006). Constitutive expression exposes functional redundancy between the *Arabidopsis* histone H2A gene *HTA1* and other H2A gene family members. *Plant Cell* **18**: 1575–1589.
- Yi, H.C., Mysore, K.S., and Gelvin, S.B.** (2002). Expression of the *Arabidopsis* histone *H2A-1* gene correlates with susceptibility to *Agrobacterium* transformation. *Plant J.* **32**: 285–298.
- Zhu, Y., et al.** (2003). Identification of *Arabidopsis rat* mutants. *Plant Physiol.* **132**: 494–505.